Int J Adv Manuf Technol (2009) 40:286–296
DOI 10.1007/s00170-007-1325-0

ORIGINAL ARTICLE

Effect of welding processes on tensile properties of AA6061 aluminium alloy joints

A. K. Lakshminarayanan · V. Balasubramanian · K. Elangovan

Received: 1 June 2007 / Accepted: 19 November 2007 / Published online: 18 December 2007

Abstract The present investigation is aimed at to study the effect of welding processes such as GTAW, GMAW and FSW on mechanical properties of AA6061 aluminium alloy. The preferred welding processes of these alloys are frequently gas tungsten arc welding (GTAW) and gas metal arc welding (GMAW) due to their comparatively easier applicability and better economy. In this alloy, the weld fusion zones typically exhibit coarse columnar grains because of the prevailing thermal conditions during weld metal solidification. This often causes inferior weld mechanical properties and poor resistance to hot cracking. Friction stir welding (FSW) is a solid phase welding technique developed primarily for welding metals and alloys that heretofore had been difficult to weld using more traditional fusion techniques. Rolled plates of 6 mm thickness have been used as the base material for preparing single pass butt welded joints. The filler metal used for joining the plates is AA4043 (Al-5Si (wt%)) grade aluminium alloy. In the present work, tensile properties, micro hardness, microstructure and fracture surface morphology of the GMAW, GTAW and FSW joints have been evaluated, and the results are compared. From this investigation, it is found that FSW joints of AA6061 aluminium alloy showed superior mechanical properties compared with GTAW and GMAW joints, and this is mainly due to the formation of very fine, equiaxed microstructure in the weld zone.

Keywords AA6061 aluminium alloy · Gas metal arc welding · Gas tungsten arc welding · Friction stir welding · Tensile properties

A. K. Lakshminarayanan · V. Balasubramanian (✉)
Center for Materials Joining Research (CEMAJOR),
Department of Manufacturing Engineering, Annamalai University,
Annamalainagar 608 002 Tamil Nadu, India
e-mail: visvabalu@yahoo.com

K. Elangovan
Department of Mechanical & Production Engineering,
Sathyabama University,
Chennai, Tamil Nadu, India

1 Introduction

Aluminium alloys find wide applications in aerospace, automobile industries, railway vehicles, bridges, offshore structure topsides and high speed ships due to its light weight and higher strength to weight ratio. In all cases, welding is the primary joining method which has always represented a great challenge for designers and technologists. As a matter of fact, lots of difficulties are associated with this kind of joint process, mainly related to the presence of a tenacious oxide layer, high thermal conductivity, high coefficient of thermal expansion, solidification shrinkage and, above all, high solubility of hydrogen, and other gases, in the molten state [1]. Further problems occur when attention is focused on heat-treatable alloys, since heat, provided by the welding process, is responsible for the decay of mechanical properties, due to phase transformations and softening [2]. AA6061 aluminium alloy (Al- Mg-Si alloys) is the most widely used medium strength aluminium alloy, and has gathered wide acceptance in the fabrication of light weight structures [3]. The preferred welding processes for these alloys are frequently gas tungsten arc welding (GTAW) and gas metal arc welding (GMAW) due to their comparatively easier applicability and better economy [4]. Welding of these alloys, however, still remains a challenge. Apart from softening in the weld fusion zone and heat-

affected zone, hot cracking in the weld can be a serious problem [5]. Friction stir welding (FSW) is an innovative solid phase welding process in which the metal to be welded is not melted during welding, thus the cracking and porosity often associated with fusion welding processes are eliminated [6]. Therefore, the FSW process can also be used to weld heat-treatable aluminum alloys in order to obtain high-quality joints. However, earlier studies [7–9] on the microstructural characteristics and mechanical properties of the friction-stir-welded joints have indicated that FSW gives rise to softening in the joints of the heat-treatable aluminum alloys such as 7075-T651 and 7475-T76 because of the dissolution or growth of strengthening precipitates during the welding thermal cycle, thus resulting in the degradation of mechanical properties of the joints. Stefano Maggiolino et al. [10] reported a comparative study on the corrosion resistance of AA6060-T5 and AA6082T6 jointed surfaces via FSW and GMAW process respectively and found friction stir welded sample has a better behaviour concerning the pitting corrosion than that of the GMAW sample. Moreira et al. [11] investigated the contrasting difference of fatigue behaviour of joints made from the traditional process of metal inert gas (MIG) welding, and the emerging process of friction stir welding. They reported that MIG and FS welded samples have a tensile strength of 65% and 70% of the base material respectively. Squillace et al. [12] proposed a comparison on electrochemical properties of gas tungsten arc welded and friction stir welded butt joints. Cabello Munoz et al. [13] investigated the microstructural and mechanical properties of friction stir welded and gas tungsten arc welded Al-Mg-Sc alloy and reported that the yield strength of friction stir welded and gas tungsten arc welded joints are decreased 20% and 50 % respectively compared to the base metal. However, no systematic study and detailed comparison has been reported on the mechanical properties of GMAW, GTAW and FSW joints of AA6061 aluminium alloy. Hence, in this investigation, an attempt has been made to evaluate the mechanical properties of GMAW, GTAW and FSW joints of AA6061 alloy.

2 Experimental work

The rolled plates of AA6061 aluminium alloy were machined to the required dimensions (300 mm×150 mm). Single 'V' butt joint configuration, as shown in Fig. 1a, was prepared to fabricate GTA and GMA welded joints. The initial joint configuration was obtained by securing the plates in position using tack welding for GTA and GMA welds. The direction of welding was normal to the rolling direction. All necessary care was taken to avoid joint distortion, and the joints were made with suitable clamps.

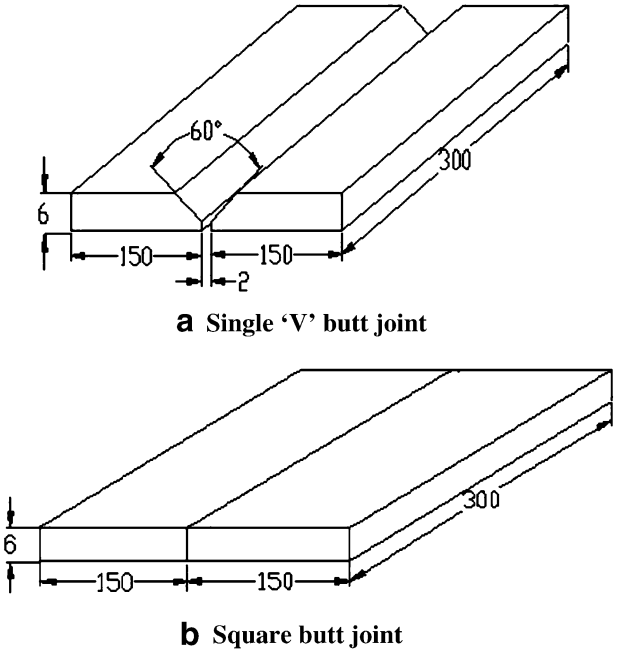

Fig. 1 Dimensions of joint configuration

Single pass welding was used to fabricate the joints. AA4043 (Al-5%Si) grade filler rod and wire were used for GTA and GMA welding processes, respectively. High purity (99.99%) argon gas was the shielding gas. Square butt joint configuration as shown in Fig. 1b was prepared to fabricate FSW joints. A non-consumable, rotating tool made of high carbon steel was used to fabricate FSW joints. The friction stir welding process is dominated by the effects associated with material flow and large mechanical deformation, which in turn is affected by process parameters such as rotational speed, welding speed and axial force. Compared to fusion welding processes, there is no porosity or other defects related to fusion. However, the hardening precipitates responsible for the good mechanical properties of heat treatable aluminium alloy are shown to be very affected by this process, partly because of their low stability. The process parameters must be optimized to get defect free joints. From the previous work done in our laboratory [14, 15], the optimum friction stir welding process parameter for joining AA6061 aluminium alloy are 1200 rpm, 1.25 mm/s (75 mm/min) and 7 kN. Trial experiments and macrostructural analysis (to identify any visible defects) were carried out for each mentioned process to find out the optimum process parameters. The welding conditions and optimized process parameters presented in Table 1 were used to fabricate the joints. Subsize cylindrical tensile specimens were prepared from the weld metal region (longitudinal direction) alone as per the ASTM E8M-04 standard to evaluate all weld metal tensile properties. The

Table 1 Welding conditions and process parameters

Process	GMAW	GTAW	FSW
Welding machine	Lincoln, USA	Lincoln, USA	RV Machine Tools, India
Tungsten electrode diameter (mm)	–	3	–
Filler rod/wire diameter (mm)	1.6	3.0	–
Voltage (volts)	20	20	–
Current (amps)	190	175	–
Welding speed (mm/min)	110	130	75
Heat input (kJ/mm)	2.021	1.212	0.84
Shielding gas	Argon	Argon	–
Gas flow rate (lit/min)	16	16	–
Tool rotational speed (rpm)	–	–	1200
Axial force (kN)	–	–	7
Tool pin profile	–	–	Threaded
Tool shoulder diameter (mm)	–	–	18
Pin diameter (mm)	–	–	6
Pin length (mm)	–	–	5.5

chemical composition and mechanical properties of base metal and weld metals are presented in Tables 2 and 3.

The welded joints were sliced (as shown in Fig. 2a) using a power hacksaw and then machined to the required dimensions as shown in Fig. 2b,c. American Society for Testing of Materials (ASTM E8M-04) guidelines were followed for preparing the test specimens. Two different tensile specimens were prepared to evaluate the transverse tensile properties. The smooth (unnotched) tensile specimens were prepared to evaluate yield strength, tensile strength, elongation and reduction in cross sectional area. Notched specimens were prepared to evaluate notch tensile strength and notch strength ratio of the joints. Tensile testing was carried out using a 100 kN, electro-mechanical controlled Universal Testing Machine (Make: FIE-Bluestar, India; Model: UNITEK-94100). The 0.2% offset yield strength was derived from the load-displacement diagram. Vicker's microhardness tester (Make: Shimadzu, Japan and Model: HMV-2T) was used for measuring the hardness of the weld metal with a 0.05 kg load. Microstructural examination was carried out using a light optical microscope (Make: MEJI, Japan; Model: MIL-7100) incorporated with an image analyzing software (Metal Vision). The specimens for metallographic examination were sectioned to the required sizes from the joint comprising weld metal, HAZ and base metal regions and polished using different grades of emery papers. Final polishing was done using the diamond compound (1 μm particle size) in the disc polishing machine. Specimens were etched with Keller's reagent to reveal the micro and macrostructure.

3 Results

3.1 Tensile properties

The transverse tensile properties such as yield strength, tensile strength, percentage of elongation, notch tensile strength, and notch strength ratio of AA6061 aluminium alloy joints were evaluated. In each condition, three specimens were tested, and the average of the three results is presented in Table 4. The yield strength and tensile strength of unwelded parent metal are 302 MPa and 335 MPa, respectively. However, the yield strength and tensile strength of GMAW joints are 141 MPa and 163 MPa, respectively. This indicates that there is a 51% reduction in strength values due to GMA welding. Similarly, the yield strength and tensile strength of GTAW joints are 188 MPa and 211 MPa, respectively which are 37% lower compared to parent metal. However, the yield strength and tensile strength of FSW joints are 224 MPa and 248 MPa, respectively. Of the three types of welded joints, the joints fabricated by FSW process exhibited higher strength values, and the enhancement in strength value is approximately 34%

Table 2 Chemical composition (wt %) of base metal and all weld metals

Type of Material	Mg	Si	Fe	Cu	Cr	Mn	Zn	Ti	Al
Base Metal (AA 6061-T6)	0.9	0.62	0.33	0.28	0.17	0.06	0.02	0.02	Bal
Weld metal (GTAW)	0.05	5.0	0.05	0.12	–	0.22	–	–	Bal
Weld metal (GMAW)	0.04	5.0	0.06	0.10	–	0.20	–	–	Bal
Weld metal (FSW)	0.8	0.60	0.35	0.26	0.19	0.08	0.01	0.01	Bal

Table 3 Mechanical properties of base metal and all weld metals

Type of Material	Yield Strength (MPa)	Ultimate Tensile Strength (MPa)	Elongation (%)	Reduction in cross sectional area (%)	Hardness (VHN)
Base Metal (AA 6061)	302	334	18	12.24	105
Weld Metal (GTAW)	160	230	8	5.45	65
Weld Metal (GMAW)	150	220	6	4.5	60
Weld metal (FSW)	245	295	14	10.2	85

compared to GMAW joints and 15% compared to GTAW joints.

Elongation and reduction in the cross-sectional area of the unwelded parent metal are 18% and 12.24%, respectively. However, the elongation and reduction in the cross-sectional area of GMAW joints are 8.4% and 5.8%, respectively. This suggests that there is a 53% reduction in ductility due to GMA welding. Similarly, the elongation

Fig. 2 Dimensions of tensile specimen

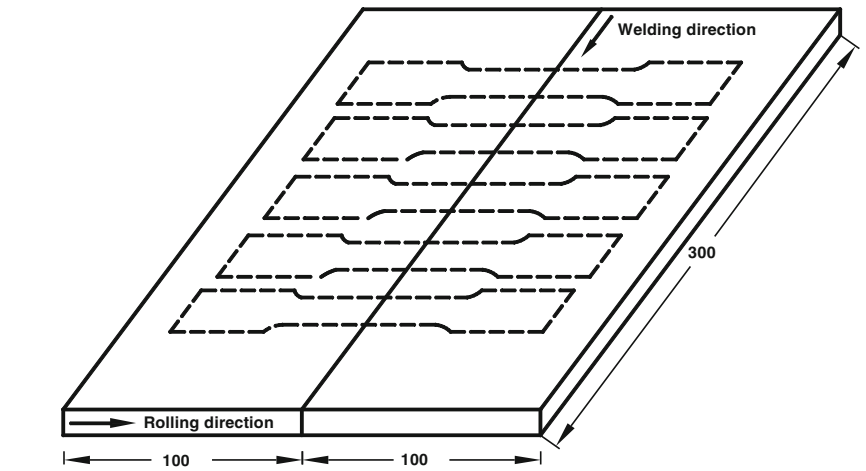

a Scheme of welding with respect to rolling direction and extraction of tensile specimens

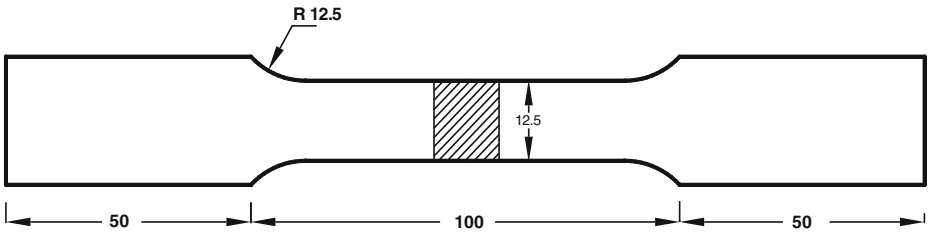

b Dimensions of flat smooth tensile specimen

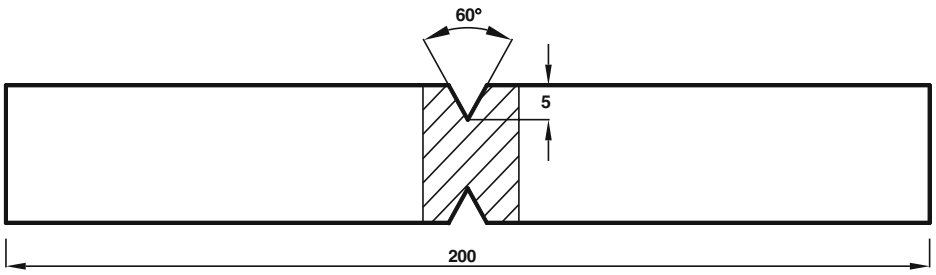

c Dimensions of flat notch tensile specimen

ASTM E8M-04 **All dimensions are in 'mm'**

Table 4 Transverse tensile properties of welded joints

Joint Type	Yield strength (MPa)	Ultimate tensile strength (MPa)	Elongation (%)	Reduction in c.s.a (%)	Notch tensile strength (MPa)	Notch strength ratio (NSR)	Joint Efficiency (%)	Weld region hardness (VHN)
GMAW	141	163	8.4	5.80	175	1.073	48.80	58
GTAW	188	211	11.8	8.26	228	1.091	62.57	70
FSW	224	248	14.2	9.56	279	1.125	74.25	85

and reduction in the cross-sectional area of GTAW joints are 11.8% and 8.26%, respectively, which are 34% lower compared to the parent metal. However, the elongation and reduction in the cross-sectional area of FSW joints are 14.2% and 9.56%, respectively. Of the three types of welded joints, the joints fabricated by FSW exhibited higher ductility values, and the improvement in ductility is approximately 41% compared to GMAW joints and 17% compared to GTAW joints.

Notch tensile strength (NTS) of unwelded parent metal is 386 MPa. However, the notch tensile strength of a GMAW joint is 175 MPa. This reveals that the reduction in NTS is approximately 55% due to GMA welding. Similarly, the NTS of GTAW is 228 MPa and the NTS of FSW is 279 MPa. Of the three types of welded joints, the joints fabricated by FSW exhibited higher NTS values, and the enhancement is 37% compared to GMAW and 18% compared to GTAW. Another notch tensile parameter, NSR, is found to be greater than unity (>1) for all the joints. This suggests that the AA6061 alloy is insensitive to notches and it is a "notch ductile materials". The NSR is 1.15 for unwelded parent metal, but it is 1.07 and 1.09 for GMAW and GTAW joints respectively. Of the three types of welded joints, the joints fabricated by FSW exhibited a relatively higher NSR (1.13), and the improvement in NSR is 5.2% compared to GMAW and 3.5% compared to GTAW process.

Joint efficiency is the ratio between tensile strength of welded joint and tensile strength of the unwelded parent metal. The joint efficiency of GMAW joints is approximately 49% and the joint efficiency of GTAW joints is 63%. Of the three types of welded joints, the joints fabricated by FSW exhibited a relatively higher joint efficiency (74%), and the joint efficiency is 34% higher compared to the GMAW joints and 15% higher compared to GTAW joints.

3.2 Hardness

The hardness across the weld cross section was measured using a Vickers Micro-hardness testing machine, and the values are presented in Table 4. The hardness of base metal (unwelded parent metal) in its initial T_6 condition is 105 VHN. However, the hardness of the GMAW and GTAW joints in the weld metal region is 58 VHN and 70 VHN respectively. This suggests that the hardness is reduced by 47 VHN and 35 VHN in the weld metal region of GMAW and GTAW joints, respectively due to welding heat and the usage of lower hardness filler metal (Al-5%Si). However, the FSW process increases the hardness to some extent in the weld metal region, and the hardness of the FSW joints in the weld metal region is 85 VHN. The hardness of FSW is 85 VHN, which is relatively higher, compared to GMAW and GTAW joints, and compared with the parent metal, the hardness is reduced by 20 VHN. This may be due to dissolution or growth of strengthening precipitates during the welding thermal cycle. However FSW exhibited higher hardness compared to GMAW and GTAW joints due to shear stresses induced by tool motion which lead to the generation of a very fine grain structure, which allows a partial recovery of hardness values.

3.3 Microstructure

Microstructure of all the joints was examined at different locations, but most of the tensile specimens failed in the weld metal region, and the optical micrographs taken at the weld metal region alone are displayed in Fig. 3 for comparison purpose. The base metal contains coarse and elongated grains with uniformly distributed very fine precipitates (Fig. 3a). The fusion zone of GMAW (Fig. 3b) and GTAW (Fig. 3c) joints contain dendritic structure and this may be due to the fast heating of base metal and fast cooling of molten metal due to welding heat. The only difference between these two dendritic structures is the dendrite arm spacing. The spacing is marginally wider in GMAW joint and narrower in GTAW joint. However, the weld region of FSW joint (Fig. 3d) contains very fine, equiaxed grains and this may be due to the dynamic recrystallisation that occurred during FSW process. Macrostructure of the joints are displayed in Fig. 4.

3.4 Fracture surface

The tensile specimen, before and after testing, are displayed in Fig. 5. In all the specimens, the location of failure is in

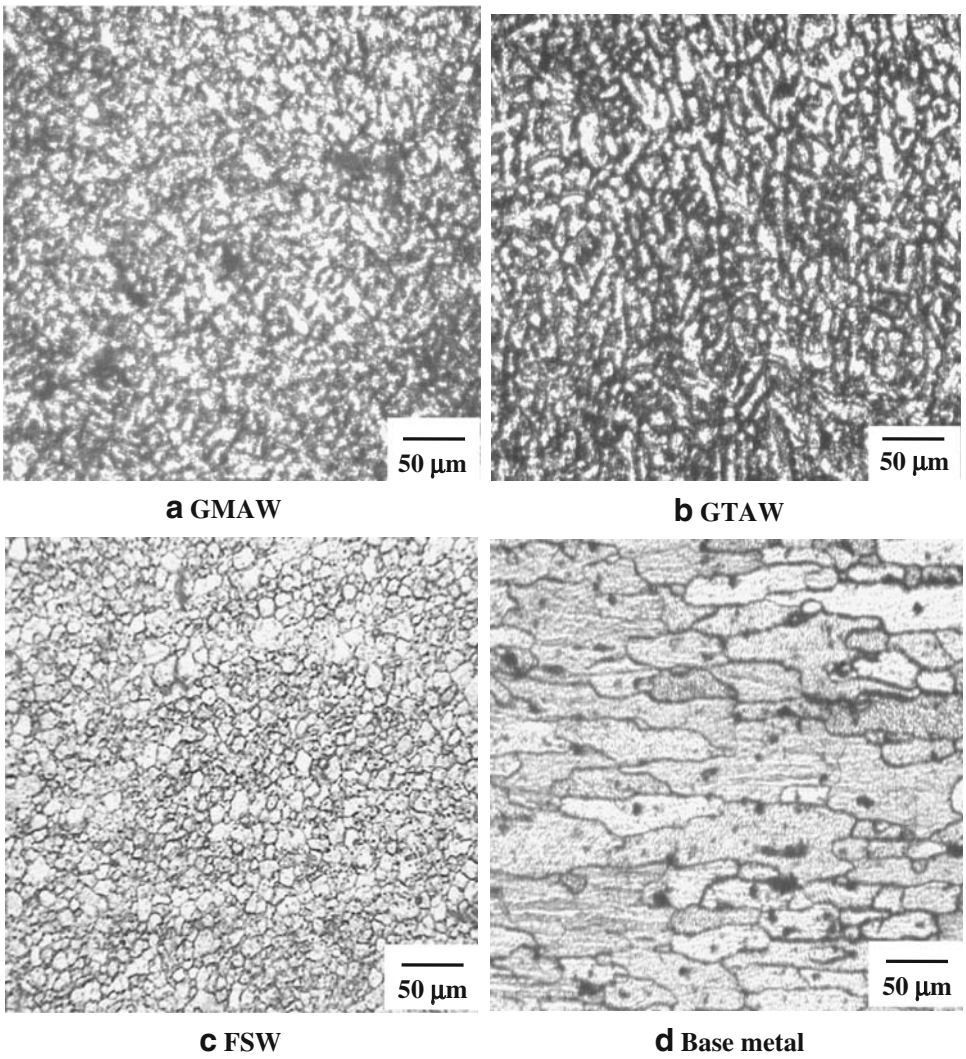

Fig. 3 Optical micrographs of weld metal region

the weld metal region only. The fractured surface of tensile specimens of welded joints was analyzed using SEM to reveal the fracture surface morphology. Figures 6 and 7 display the fractographs of unnotched and notched tensile specimens, respectively. The displayed fractographs invariably consist of dimples, which are an indication that most of the tensile specimens failed in a ductile manner under the action of tensile loading. An appreciable difference exists in the size of the dimples with respect to the welding processes. An intergranular fracture feature has been observed in GMAW joints (Figs. 6a and 7a). This may be due to the combined influence of a coarse grained weld metal region and a higher amount of precipitate formation at the grain boundaries. Coarse dimples are seen in GTAW joints (Figs. 6b and 7b) and fine dimples are seen in FSW joints (Figs. 6c and 7c). Since fine dimples are a characteristic feature of ductile fracture, the FSW joints have shown higher ductility compared to all other joints (Table 4). The dimple size exhibits a directly proportional relationship with strength and ductility, i.e., if the dimple size is finer, then the strength and ductility of the respective joint is higher and vice versa [16].

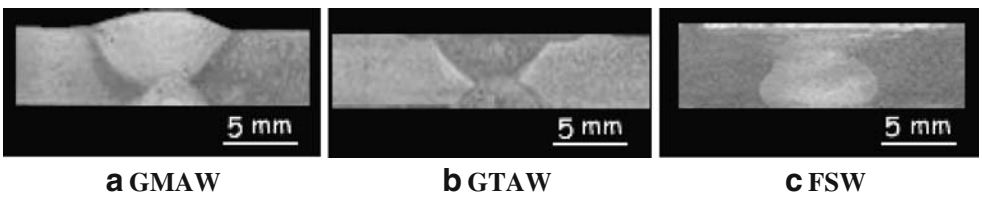

Fig. 4 Macrostructure of welded joints

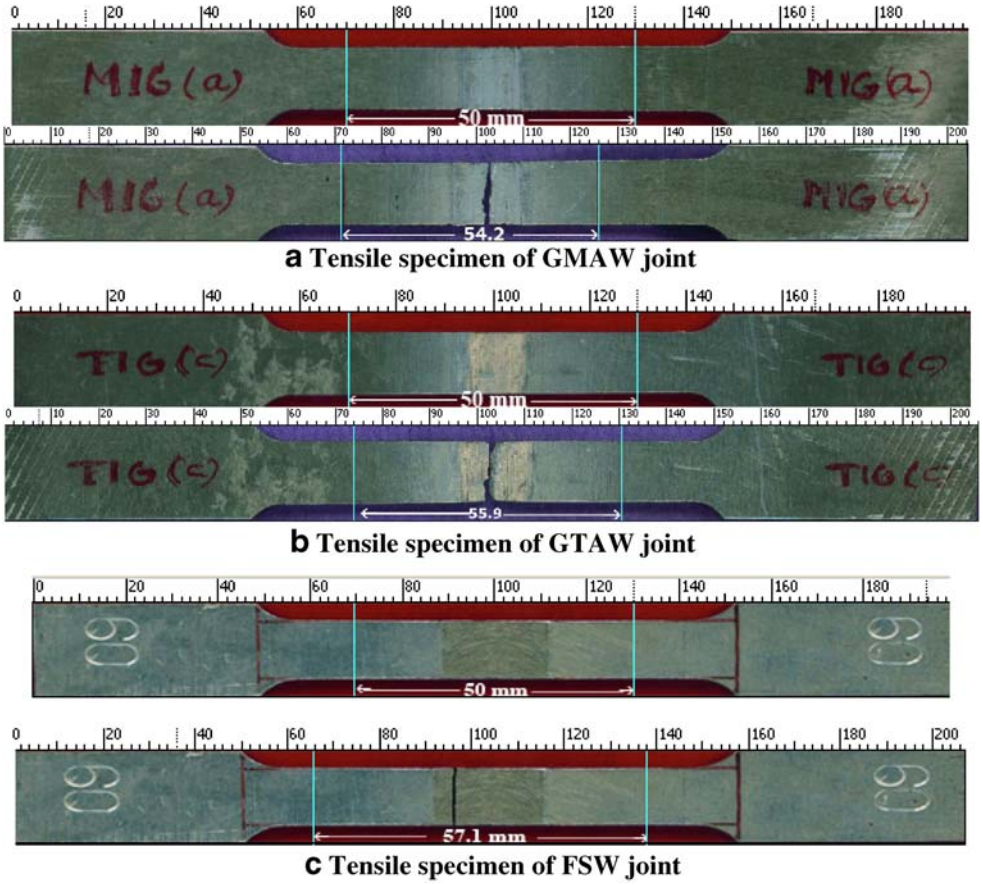

Fig. 5 Fracture location of tensile specimens

4 Discussion

Transverse tensile properties of the welded joints presented in Table 4 indicate that the FSW joints are exhibiting superior tensile properties compared to GMAW and GTAW joints. During tensile test, all the specimens invariably failed in the weld region (Fig. 4). This indicates that the weld region is comparatively weaker than other regions and hence the joint properties are controlled by weld region chemical composition and microstructure.

The higher strength of the base metal is mainly attributed to the presence of alloying elements such as silicon and magnesium and these two elements combine and undergo precipitation reaction and form a strengthening precipitate of Mg_2Si. Fine and uniform distribution of these precipitates throughout the aluminium matrix provides higher strength and hardness to these alloys [17]. When these alloys are welded using non-heat treatable filler metals (Al-5%Si) to avoid solidification cracking problem, the weld region is composed of fewer Mg_2Si precipitates when compared to base metal [18]. In fusion welding, the dilution of base metal in weld metal is a common phenomenon. Even though, a large amount of silicon is available (available in base metal and filler metal) for precipitation reaction, the available magnesium (available in base metal alone) in the molten weld pool for the precipitation reaction is very low. Hence, the weld region of AA6061 aluminium alloy, when welded with AA4043 filler metal usually contains a lower amount of Mg_2Si precipitates compared to the base metal region. In the weld region of GMAW and GTAW joints, there is a depletion of Mg_2Si precipitates due to above said reasons [19]. On the other hand, the weld region of the FSW joint contains the alloying elements similar to that of base metal (Table 1a). In FSW, there is no filler metal addition, and there is no melting of base metal. Hence there is no dilution of alloying elements in the weld region. The base metal is plastically stirred under the action of the rotating tool. Due to this severe plastic deformation, the coarse elongated grains are fragmented into fine, equiaxed grains, and coarse strengthening precipitates are fractured into very fine uniformly distributed particles in the friction stir processed zone [20]. Ying chun chen et al., [19] opined that during higher rotation speeds, particles would suffer more fragmentation. The metastable precipitates will be dissolved and solutionized in the aluminium matrix during FSW, but the stable precipitates remained and are prone to segregate in the high-strain region [21]. Fonda et al. [22] reported that as the rotational speed increased, and the temperature within the nugget becomes higher and more uniform, the volume fraction of coarse second phase

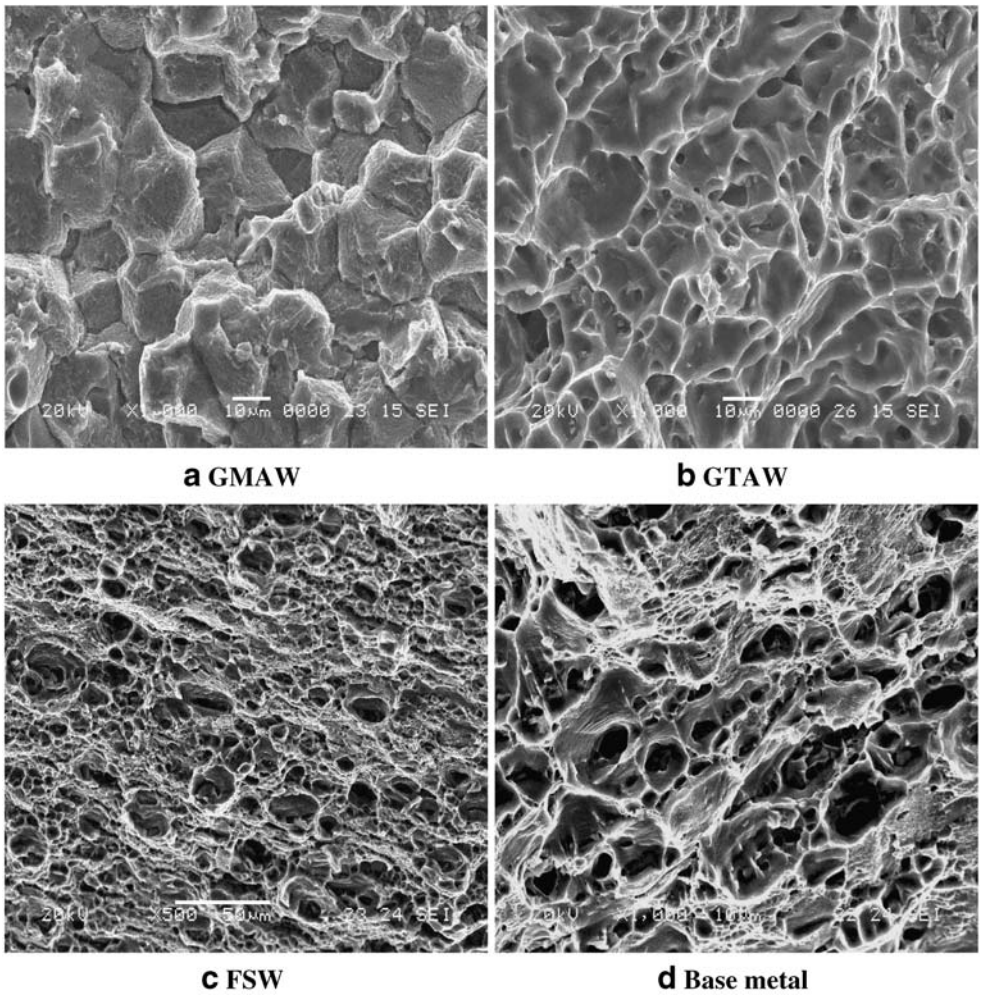

Fig. 6 SEM fractographs of smooth tensile specimen

particles decreased at different positions within the nugget zone region. The fracture location therefore corresponds to the region with the least precipitate strengthening. As the peak temperature during FSW was about 400°C for this alloy and was not sufficient to force stable precipitates to dissolve and solutionize into the aluminium matrix. In the weld region of FSW joints, there is no possibility of depletion of Mg_2Si precipitates as in the case of GMAW and GTAW joints.

The grain size of the weld region also plays a major role in deciding the joint properties. The grain size of the weld region is influenced by the heat of the welding process. Of the three welding processes used in this investigation to fabricate the joints, the GMAW process has higher heat input compared to the GTAW and FSW processes [23]. Since GMAW is a consumable electrode process, the filler metal is always connected to positive (reverse) polarity of the direct current (DCRP). This leads to a large amount of heat generation (approximately two-thirds of total heat generation) at the filler metal end. Further, a current of 190 A is passing through a small diameter of filler metal (1.6 mm), and the current density is very high in the GMAW process. Much heat generation and very high current density combine to enhance the arc temperature and arc forces [24]. Very high arc temperature increases the peak temperature of the molten weld pool causing a slow cooling rate. This slow cooling rate, in turn, causes relatively wider dendritic spacing in the fusion zone. These microstructures generally offer lower resistance to indentation and deformation and this may be one of the reasons for lower hardness and inferior tensile properties of GMAW joints.

In GTAW, the alternating current (AC) polarity is used, and the high heat generation end is continuously changing (50 times in one second). Whenever, the electrode becomes positive, more heat is generated (two-thirds of total heat) at this end. Similarly, whenever the workpiece becomes positive, more heat is generated at this end. In one half of a cycle, electrode attains maximum heat and in the other half of a cycle, the workpiece attains minimum heat, and this will change in the next cycle [25]. So, while using alternating current, the maximum heat generation end is not fixed as in the case of GMAW. However, in both processes, the heat energy from the arc is utilized to melt the filler

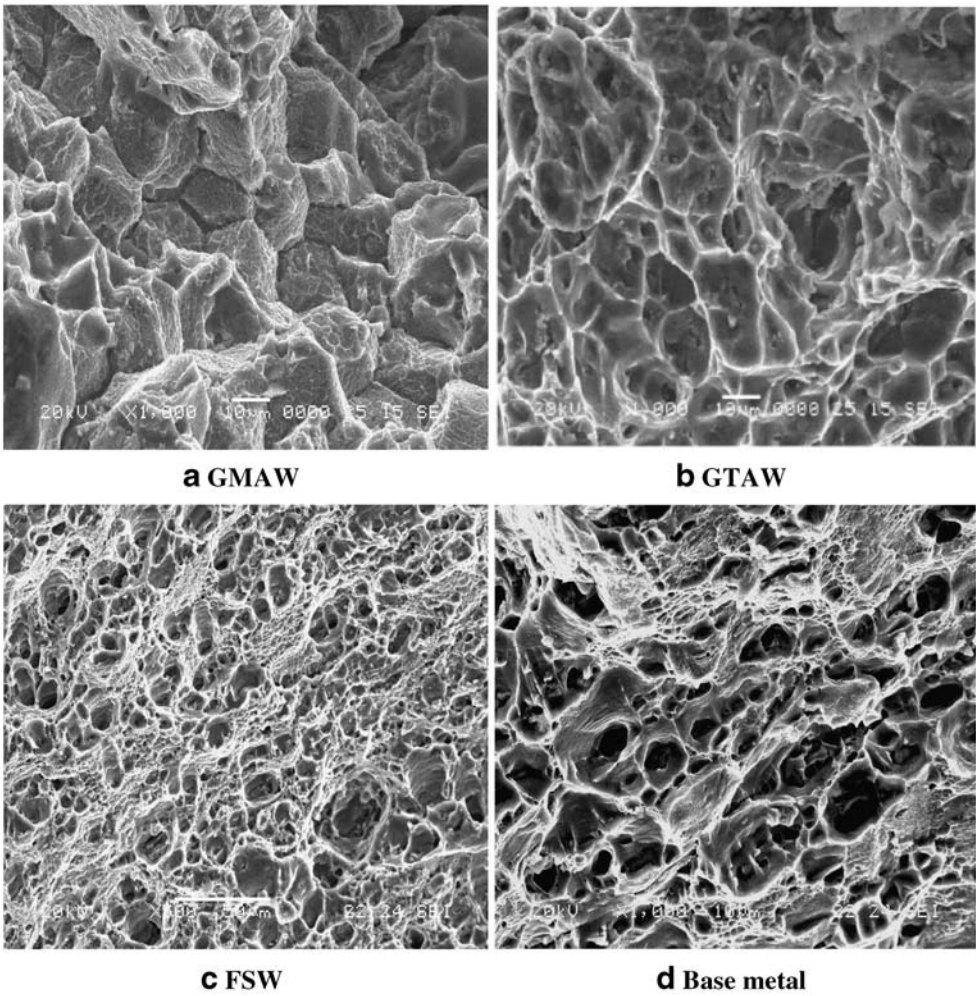

Fig. 7 SEM fractographs of notched tensile specimen

metal as well as to melt the base metal. However in GTAW, the filler rod is melted in the plasma region of the arc (midway between positive and negative polarity) and not in the positive polarity as in the case of GMAW. Due to this reason, heat input of GTAW is lower than for GMAW. Lower heat input and lower current density reduces the arc temperature and arc forces in GTAW [26]. Lower arc temperature reduces the peak temperature of the molten weld pool causing fast cooling. This fast cooling rate, in turn, causes relatively narrower dendritic spacing in the fusion zone. These microstructures generally offer improved resistance to indentation and deformation and this may be one of the reasons for higher hardness and superior tensile properties of GTAW joints compared to GMAW joints.

In FSW, the heat generation beneath the rotating tool is always in the order of 400°C and hence there is no possibility of formation of a molten weld pool [27]. Tang et al. [28] reported that when the process parameters are changed, the temperature field was then changed simultaneously. However, the variations of the temperature values are limited by the melting point of the welding material and the maximum temperature ranges from 80% to 90% of the melting point. It implies that the variation of process parameters does not affect the temperature field significantly although a relation between the temperature field and process parameters exists [29]. Colegrove et al. [30] opined that the effect of changing the welding or rotation speeds on the peak temperature is small, for conditions that produce sound welds. Zhang et al. [31] investigated the effect of axial pressure in friction stir welding of AA6061 aluminium alloy and reported that the maximum temperature and plastic contribution to the temperature field can be increased with an increase in the axial pressure. Due to the frictional heat generated between the tool shoulder and the base metal, the material under the action of the rotating tool attains a plastic state. The axial force applied through the rotating tool causes the plasticized metal to extrude around the tool pin in the vertical direction and get consolidated in the back side when the tool moves forward. Both the stirring and extrusion causes the elongated grains to fragment into smaller grains and fractures the strengthening precipitates into very fine particles.

Su et al. [32] confirmed that during FSW the original base metal grain structure is completely eliminated and replaced by a very fine equiaxed grain structure in the FSP zone. They opined that it was unlikely that the dynamic recrystallisation occurred via a conventional discontinuous process during FSW. In the more conventional context, recrystallisation proceeds by nucleation and growth of new grains surrounded by high angle boundaries. However, the microstructural evidence in their study did not support conventional grain nucleation with high angle grain boundaries, nor grain boundary migration as required by a discontinuous dynamic recrystallisation mechanism. Rather, it appeared that a continuous dynamic recrystallisation process was the primary mechanism. In friction stir processed (FSP) AA 7075 alloy, Ma and Mishra [33] made three important observations using TEM micrographs: (i) the fine precipitates were uniformly distributed within the interior of grains and at the grain boundaries (ii) while the grain boundary particles usually exhibited a needle or disc type morphology, the precipitates inside the grains generally had an equiaxed shape; (iii) the precipitates in the FSP zone were fine and generally had a size of <0.5 μm. This may be one of the reasons for superior tensile properties of FSW joints compared to GMA and GTA welded joints.

5 Conclusions

In this paper, the mechanical properties of GMAW, GTAW and FSW joints of AA6061 aluminum alloy were evaluated. From this investigation, the following important conclusions have been derived:

(i) Of the three welded joints, the joints fabricated by FSW process exhibited higher strength values and the enhancement in strength value is approximately 34% compared to GMAW joints, and 15% compared to GTAW joints.
(ii) Hardness is lower in the weld metal (WM) region compared to the HAZ and BM regions irrespective of welding technique. Very low hardness is recorded in the GMAW joints (58 VHN) and the maximum hardness is recorded in the FSW joints (85 VHN).
(iii) The formation of fine, equiaxed grains and uniformly distributed, very fine strengthening precipitates in the weld region are the reasons for superior tensile properties of FSW joints compared to GTAW and GMAW joints.

Acknowledgements The authors are grateful to the Department of Manufacturing Engineering, Annamalai University, Annamalainagar, Tamil Nadu, India for extending the facilities of Metal Joining Laboratory and Materials Testing Laboratory to carryout this investigation. The authors also wish to express their sincere thanks to Aeronautical Research & Development Board (ARDB), Ministry of Defence, New Delhi for the financial support to carryout this investigation through sponsored project No.DARO/08/1061356/M/I.

Appendix-1

Heat input calculations of processes used

Gas metal arc welding

$$Heat\ Input = \frac{V \times I \times \eta \times 60}{S \times 1000} = \frac{190 \times 20 \times 0.75 \times 60}{110 \times 1000} = 2.021\ \text{kJ/mm}$$

Gas tungsten arc welding

$$Heat\ Input = \frac{V \times I \times \eta \times 60}{S \times 1000} = \frac{175 \times 20 \times 0.75 \times 60}{130 \times 1000} = 1.212\ kJ/mm$$

Where V - Voltage in volts, I - Current in Amps, η - Arc efficiency is assumed as 0.75 for GMAW and GTAW [34]

Friction stir welding

The heat input for friction stir welding process can be calculated as [35]

$$q = \frac{2\pi}{3S} \times \mu \times p \times \omega \times R_S \times \eta = \frac{2\pi}{3 \times 1.25} \times 0.3 \times 7 \times 26.6 \times 0.009 \times 0.8 = 0.84\ KJ/mm$$

Where,

μ - Co-efficient of friction , P - Normal force in kN, ω - Rotational speed in rev/sec

R_s - Shoulder radius in m, S - Welding speed in mm/s.

References

1. Matrukanitz RP (1990) Selection and weldability of heat-treatable aluminum alloys. ASM Handbook-Welding, Brazing and Soldering 6:528–536
2. Senthil Kumar T, Balasubramanian V, Sanavullah MY (2007) Influences of pulsed current tungsten inert gas welding parameters on tensile properties of AA6061 aluminium alloy. Mater Des 28 (7):2080–2092
3. Balasubramanian V, Ravisankar V, Madhusudhan Reddy G (2007) Effect of pulsed current welding on mechanical properties of high strength aluminium alloy. Int J Adv Manuf Technol (in press)
4. Madhusudhan Reddy G, Gokhale AA, Prasad Rao K (1998) Optimization of pulse frequency in pulsed current gas tungsten arc welding of aluminium – lithium. J Mater Sci Technol 14:61–66
5. Mohandoss T, Madhusudhan Reddy G (1996) Effect of frequency of pulsing in gas tungsten are welding on the microstructure and mechanical properties of titanium alloy welds. J Mater Sci Lett 15:626–628
6. Knipstrom KE, Pekkari B (1997) Friction stir welding process goes commercial. Weld J 76:55–57

7. Mahoney MW, Rhodes CG, Flintoff JG, Spurling RA, Bingel WH (1998) Properties of friction stir welded 7075-T651 aluminum. Metallurgical Mater Trans A 29:1955–1964
8. Campbell G, Stotler T (1999) Friction stir welding of armor grade aluminum plate. Weld J 78:45–47
9. Liu HJ, Fujii H, Maeda M, Nogi (2003) Tensile properties and fracture locations of friction stir welded joints of 2024-T351 aluminium alloy. J Mater Process Technol 36:402–408
10. Maggiolino S, Schmid C (2007) Corrosion resistance in FSW and in MIG welding techniques of AA6XXX. J Mater Process Technol (in press)
11. Moreira PMGP, de Figueiredo MAV, de Castro PMST (2007) Fatigue behaviour of FSW and MIG weldments for two aluminium alloys. Theor Appl Fract Mech 48:169–177
12. Squillace A, De Fenzo A, Giorleo G, Bellucci F (2004) A comparison between FSW and TIG welding techniques: modifications of microstructure and pitting corrosion resistance in AA 2024-T3 butt joints. J Mater Process Technol 152:97–105
13. Munoz C, Ruckert G, Huneau B, Sauvage X, Marya S (2004) Comparison of TIG welded and friction stir welded Al-4.5 Mg-0.26 Sc alloy. J Mater Process Technol 152:97–105
14. Elangovan K, Balasubramanian V, Valliappan M (2007) Influences of tool pin profile and axial force on the formation of friction stir processing zone in AA6061 aluminium alloy. Int J Adv Manuf Technol (in press). DOI 10.1007/s00170-007-1100-2
15. Elangovan K, Balasubramanian V (2008) Influences of tool pin profile and tool shoulder diameter on the formation of friction stir processing zone in AA6061 aluminium alloy. Mater Des 29 (2):362–373
16. Lin DC, Wang TS, Srivatsan TS (2003) A mechanism for the formation of equiaxed grains in welds of aluminum-lithium alloy 2090. Mater Sci Eng A 335:304–309
17. Mondolfo LF (1997) Aluminium alloys - structure and properties. Butterworths, London
18. Shinoda T, Ueno Y, Masumoto I (1990) Effect of pulsed welding current on solidification cracking in austenitic stainless steel welds. Trans Jpn Weld Soc 21:18–23
19. Madhusudhan Reddy G, Gokhale AA, Prasad Rao K (1997) Weld microstructural refinement in a 1441 grade Al-Li alloy. J Mater Sci 32:4117–4126
20. Kwon YJ, Shigematsu I, Saito N (2003) Mechanical properties of fine-grained aluminium alloy produced stir process. Scr Mater 9:785–789
21. Ericsson M, Sandstrom R (2003) Influences of welding speed on the fatigue of friction stir welds and comparison with MIG and TIG. Int J Fatigue 25:1379–1387
22. Ying Chun C, Huijie L, Jicai F (2006) Friction stir welding characteristics of different heat-treated-state 2219 aluminium alloy plates. Mater Sci Eng A 420:21–25
23. Fonda RW, Lambrakos SG (2002) Analysis of friction stir welds using an inverse problem approach. Sci Technol Join 7(3):177–181
24. Potluri NB, Ghosh PK, Gupta PC, Reddy YS (1996) Studies on weld metal characteristics and their influences on tensile and fatigue properties of fatigue properties of pulsed current GMA welded Al-Zn-Mg alloy. Weld J 75:62s–70s
25. Norman AF, Drazhner V, Prangnell PB (1999) Effect of welding parameters on the solidification microstructure of autogenous TIG welds in an Al-Cu-Mg-Mn alloy. Mater Sci Eng, A 259:53–60
26. Madhusudhan Reddy G, Mohandoss T, Prasad Rao K (2005) Sci Technol Weld Joining 10:121–128
27. Jata KV, Seminatin SL (2000) Continuous dynamic recrystallization during friction stir welding of high strength aluminium alloy. Scr Mater 43:743–749
28. Tang W, Guo X, McClure JC, Numes LE (1998) Heat input and temperature distribution in friction stir welding. J Mater Process Manuf Sci 7(2):163–172
29. Zhang Z, Zhang HW (2007) Material behaviors and mechanical features in friction stir welding process. Int J Adv Manuf Technol 35:86–100
30. Colegrove PA, Shercliff HR (2005) 3-Dimensional CFD modelling of flow round a threaded friction stir welding tool profile. J Mater Process Technol 169:320–327
31. Zhang Z, Zhang HW (2007) Numerical studies on effect of axial pressure in friction stir welding. Sci Technol Weld Joining 12 (3):226–248
32. Su JQ, Nelson TW, Mishra R, Mahoney M (2003) Microstructural investigation of friction stir welded 7050-T651 aluminium. Acta Mater 51:713–729
33. Ma ZY, Mishra RS (2003) Cavitation in super plastic 7075 aluminium alloys and prepared via friction stir processing. Acta Mater 51:3551–3569
34. AWS Welding Hand book (1996) 3:232–235
35. Heurtier P, Jones MJ, Desrayaud C, Driver JH, Montheillet F, Allehaux D (2006) Mechanical and thermal modelling of friction stir welding. J Mater Process Technol 171:348–357